DRA

THE CORRELATION OF STRUCTURAL, CHEMICAL, AND ELECTRONIC PROPERTIES OF SMALL METAL PARTICLES AND THEIR ALLOYS

Final Technical Report

for the Period
May 20, 1982 - July 31, 1983

Submitted to

National Aeronautics and Space Administration
Ames Research Center
Moffett Field, CA 94305

Computational Chemistry and Aerothermodynamics Branch
Dr. Jim Arnold, Chief
Dr. Helmut Poppa, Technical Monitor

Report No.:
EI 84-0408
Grant No: NCC2-193

Prepared by

ELORET INSTITUTE
1178 Maraschino Drive
Sunnyvale, CA 94087
(Phone: (408) 730-8422)
K. Heinemann, Ph.D., President

THE CORRELATION OF STRUCTURAL, CHEMICAL, AND ELECTRONIC PROPERTIES OF SMALL METAL PARTICLES AND THEIR ALLOYS

ABSTRACT

The low-pressure interaction of CO with small Ru particles supported on UHV cleaved mica has been studied using flash thermal desorption, Auger electron spectroscopy, transmission electron microscopy, and transmission electron diffraction. Average particle sizes for these experiments varied between 1.2 and 1.6 nm. A careful search for CO decomposition on the Ru particles revealed no evidence of dissociation over a temperature range and pressure range of 300 to 550 C and 10(-11) to 10(-6) millibar, respectively. Gas and heat treatments caused significant morphological changes and dispersion in the Ru particles, which affected CO desorption. These effects were dependent on the particle size.

1. INTRODUCTION

Ruthenium is an effective catalyst for a number of processes including CO methanation and Fischer-Tropsch synthesis. Thus, there has been considerable interest in CO-interaction studies on both single crystal surfaces (1-6) and supported small particles of Ru (7-8). We present results of studies of the interaction of CO with small Ru particles supported on UHV-cleaved mica, employing Flash Thermal Desorption (FTD), Auger Electron Spectroscopy (AES, Transmission Electron Microscopy (TEM), and Transmission Electron Diffraction (TED). We were particularly interested to see if during repeated CO FTD cycles, we would observe the dissociation of CO as was observed for Pd and Ni particles supported on mica (9,10). Our results showed no evidence for CO decomposition on Ru particles. However, we present evidence for significant morphology changes of particles induced by gas- and heat-treatments which affect CO desorption.

2. EXPERIMENTAL

In a dual-chamber system as previously described (9), small Ru particles were vapor grown onto high purity mica (muscovite) that was heat treated and cleaved in ultra high vacuum. During vapor deposition, the substrate temperature and metal flux were held constant at 270 C and 0.20 nm/min, respectively. The metal flux was measured with a quartz crystal microbalance positioned such that a 1 Hz decrease in the crystal oscillation frequency corresponded to 0.020 nm Ru deposited on the sample. The pressure during deposition was less than 5×10^{-9} Torr. Deposition times ranged from 30 to 300 seconds. The samples were analyzed by AES to determine the relative metal coverages and the presence of contamination. Successive flash thermal

desorptions of CO were used to observe the chemisorption properties of the particles and to assess changes which occur as a result of thermal desorption cycling and other gas-thermal treatments. All CO desorptions were accomplished by rapidly inserting the sample into a cylindrical oven which was held at a temperature of 370 C. The surface temperature versus time was approximated from earlier temperature calibrations using thermocouples imbedded into the mica (11). Desorption spectra are presented as a function of time and desorption features are characterized by temperature using this calibration. The CO desorption flux was monitored by a line-of-sight quadrupole mass spectrometer through a hole in the oven wall. Auger spectra were taken immediately after the desorption of CO (P_{CO} 1×10^{-9} Torr) to insure minimum CO coverage of the sample from background CO and prevent electron beam induced contamination of the particle surfaces. Also, the electron beam dose was minimized to avoid decomposition of the mica. After a set of samples was tested, the specimens were removed from the UHV system, thinned, and evaluated by TEM-TED.

3. RESULTS

Transmission Electron Microscopy and Diffraction: samples removed from the vacuum system "as deposited," without further gas or thermal treatments, were examined by TEM and found to have average particle diameters ranging from 1.2 to 6 nm for 30 to 300 second deposition time. Figures Ia-Id show representative micrographs for the Ru deposits. The particle number density ranged from 1.3×10^{12} to $3.7 \times 10^{12}/cm^2$. For an equivalent metal exposure, the Ru particles on mica are smaller and have a higher number density when compared with Pd/mica. This increased nucleation rate suggests an increased interaction between Ru and mica. TED patterns of all depositions were indexed with hcp structure. Structural modification to fcc which was

observed in the case of small Gd particles (12) was not detected here. TED showed that all depositions exhibited a high degree of epitaxy (see Fig. 1d). The observed epitaxial relationships, using (hk·l) indexing, were:

$$\langle 100\rangle_{Ru}//\langle 020\rangle_{mica} \quad \text{or} \quad \langle 130\rangle_{mica} \text{ and } \langle 110\rangle_{Ru}//\langle 200\rangle_{mica}$$

The particles were predominantly oriented with the Ru [001] direction normal to the mica surface. The exposed crystal faces depended on the three dimensional particle shapes which are not directly discernible from TED; from surface free energy considerations, one would expect predominantly (101) and (001) facets.

CO Desorption Spectra: Typical desorption spectra for a 25 Hz deposit as a function of CO exposure are shown in Fig. 2. When assigning a temperature scale to these curves, the shapes and changes with CO exposure are consistent with first order desorption with a coverage dependent activation energy. From the peak position of the low coverage FTD spectrum, we then calculate an activation energy of 35 kcal/mole, assuming a pre-exponential factor of 10^{+16}sec^{-1}, as suggested by H. Pfnuer, et al. (13). (If the usual factor of 10^{13}sec^{-1} is used, a E_{des} = 29 kcal/mole results.) The initial spectra for three different particle sizes and saturated CO dose (6L) are shown in Fig. 3. The increasing metal surface area produces more desorbed CO as expected. Normalizing these curves to the same peak height showed that the peak shape and positions did not differ significantly over this range of particle size. Single crystal studies of CO desorption from a number of different crystal faces show a fair amount of structure sensitivity for CO desorption peak shape. Our results, therefore, suggest that the three dimensional shapes of the particles remained relatively constant for these various conditions.

Search for CO Decomposition: A careful search for evidence of CO decomposition on small Ru particles produced by CO adsorption/desorption cycles was carried out by: a) measuring successive CO FTD spectra and looking for decay in peak height and peak area due to carbon buildup (if loss of peak area by particle sintering and/or reconstruction can be excluded), and b) performing AES measurements on the supported particles after each FTD to search for C contamination. Figure 4 shows a typical set of successive spectra recorded using 6L saturation doses of CO. Only slight asymmetric losses of area on the high temperature sides of the first few desorptions were observed. This is in contrast to previous results for Pd and Ni particles (9,10) in which 30-70% area losses were found. (In some cases we did observe a significant decay of FTD area. However, these decays were caused by small amounts of coadsorbing oxygen due to accidental small leaks in our vacuum system. Once these leaks were eliminated, all significant FTD area losses vanished.)

Evidence was also sought for particle coalescence during repeated CO FTD cycles because sintering also causes FTD peak area losses. TEM micrographs of essentially identical Ru deposits that had or had not experienced several FTD cycles were compared for this purpose. Measurements of particle size and number density showed no significant change, however. Thus, the observed small decrease in CO surface area can not be attributed to sintering. We are therefore led to the conclusion that the minor loss of FTD peak area is due only to morphological particle changes or to minor particle/support interactions that occur during CO adsorption-desorption cycling.

A careful search for the presence of carbon using high sensitivity AES was carried out although this was hampered by the well known difficulties

caused by C/Ru spectrae overlap. Difference curves of the Ru (273 eV) peak before and after several FTD cycles, as well as measuring ratios of Ru (273 eV) to Ru (231 eV) and to Ru (200 eV) peaks yielded no detectable C. In some cases, the sensitivity was high enough that 0.01 monolayer of C would have been detected. The primary conclusion of these results is that at least for the surface coverages and temperatures of our experiments, no C buildup on the Ru particles was observed within our detection limit; therefore, no CO decomposition on Ru particles was concluded to occur.

Effect of Steady State Heat Treatment: The changes induced by extended time heat treatments were examined by FTD and TEM. After a first CO FTD cycle, the sample was annealed at 350 C for 35 minutes, cooled to 50 C and a second FTD cycle was carried out. Additional anneals, each followed by a CO adsorption/desorption cycle, followed. The results for a 5 Hz deposit are shown in Fig. 5a, where a decrease in peak area with successive flashes is obvious. Note the distinct asymmetric decrease on the high energy side of the peak. This behavior suggests that annealing reduces the concentration of high energy binding sites for CO. It was also found that the rate of decay in FTD peak area with successive flashes is strongly particle size dependent as shown in Fig. 5b. As also discussed in the next section, we attribute these annealing effects to a combination of particle coalescence and faceting. The TEM evidence for the latter is very strong as seen in Fig. 6 for deposits before and after that treatment. We see that the particles are transformed from irregular shapes to well-defined hexagonal shapes. Such changes will be accompanied by a reduction in surface irregularities such as steps, kinks, edges and corners which are usually correlated with lower coordination surface atoms with higher adsorption energy.

Effect of O_2 Preexposure: When a CO FTD cycle included a 0.3 L predose of O_2 (5×10^{-9} Torr for 60 seconds) at room temperature, the resulting FTD curves (see Fig. 7) showed a clear asymmetric decrease, similar to peak decay observed upon simple annealing (see above). With increasing amount of predosed O_2, the CO FTD peak height decreased further and the peak shifted substantially towards the lower temperature side; CO adsorption eventually was totally blocked by 6L oxygen as can be seen in Fig. 7. Such a strong peak shift to lower temperature suggests a substantial decrease of CO binding energy in the remaining adsorption sites.

However, this CO peak decay was partially reversible; about 90% of the original peak area could be recovered by the standard heat treatment (300 C for 35 minutes). O_2 desorption could not occur at this temperature (the activation energy for O_2 desorption is approximately 80 kcal/mole (2,14)). Oxygen removal by background CO to form CO_2 can also be dismissed because the CO oxidation rate at 300 C and CO pressures as high as 10^{-7} Torr is still very low (14). In spite of this, an attempt was made to observe the CO_2 reaction directly by producing a high CO background pressure of 1×10^{-7} Torr during standard (300C) heat treatment, but no CO_2 was detected.

When, however, the Ru particles were exposed to oxygen at high temperature, the FTD area losses were irreversible. During an exposure of a clean Ru/mica sample to 5×10^{-9} Torr O_2 at 350 C for 35 minutes, the particles were permanently poisoned, incapable of adsorbing any CO. We suspect that the heated particles become partially oxidized when exposed to oxygen.

The TEM results for particles (see Fig. 8) heat treated in O_2 (5×10^{-9} Torr at 350 C for 30 minutes) support the surface oxidation hypothesis. All TED patterns showed Ru reflections only and no Ru-oxide rings

were detected. The possibility of bulk oxidation is, therefore, excluded. However, the oxidized particles are spreading out more over mica surface (wetting). This type of particulate surface oxidation and increased wetting of an oxide support has been reported for Ni/mica (9), Fe/Al_2O_3 (15), Pt/Al_2O_3 (16), and Ir/SiO_2 (17).

4. DISCUSSION AND CONCLUSIONS

The lack of evidence for CO decomposition at low CO pressure on Ru particles supported on mica is the same as in the case of Pt/mica (18), but contrary to what was observed for Pd/mica (10) and Ni/mica (9). The strong particle size effect seen on Pd and Ni was attributed to the high density of edge and corner sites (low coordination sites) on small particles. The same type of sites are presumably present also in high concentrations on evaporated Pt and Ru particles, yet no dissociation of CO was observed. This observation for Ru disagrees with the general criteria for predicting CO dissociation as proposed by Broden, et al. (19) wherein the transition metals are ordered according to their tendency to dissociate CO (as predicted from photoemission studies of adsorbed CO). Ni and Pd are further removed from the region of transition between low and high CO dissociation tendency than Ru. We would thus expect Ru to have a greater tendency to decompose CO than either Ni or Pd.

The pronounced particle size dependence of CO decomposition seen on Pd and Ni, and the fact that no CO decomposition has been observed on the low-index single crystal surfaces of these metals suggest that CO decomposition occurs on sites which differ substantially from those on single crystal surfaces. CO chemisorption bonding is generally explained by the donor-acceptor mechanism (Blyholder model (20,21)), in which the bond is formed through electron transfer from the highest filled orbital of CO (5σ) to the

metal and by back-donation of metal electrons to the lowest unfilled orbital of CO. This electron transfer into the $2\pi^*$ orbitals can cause appreciable weakening of the C - O bond (22). Our "special" sites could conceivably lead to CO decomposition through their greater ability to weaken the carbon-oxygen bond via an increased "back-donation" of electrons. Whether the types and numbers of such sites on small Ni, Pd, Pt, and Ru particles are of comparable nature is an open question at this point because possible differences in microstructure and habits have not been sufficiently characterized. If similar particle habit are assumed, however, the density and types of "special sites" on particles of comparable size should be similar (22). The discrepancies in the tendencies of the various group VIII metals to decompose CO would then have to be ascribed to the differing electronic structure of the various metals or to different metal/support interactions.

A survey of previous work on CO decomposition on Ru introduces another aspect of the interpretation of our results, namely, CO pressure. Goodman, et al. (4) could not detect any surface carbon after heating a Ru (110) surface to 630 K at a CO pressure of 2×10^{-3} Torr for 30 minutes, and Madey et al. (1) observed no detectable CO dissociation on Ru(001) at temperatures and pressures as high as 700 K and 10^{-4} Torr, respectively. In high pressure experiments, on the other hand, Singh and Grenga (23) have reported carbon deposition on a polycrystalline Ru sphere exposed to 760 Torr of CO at 550 K and Goodman et al. (24) more recently reported carbon deposition from CO on a Ru(110) surface exposed to 24 Torr of CO. Also Low and Bell (7) found disproportionation of CO at high pressure (1 atm) during CO desorption on supported Ru particles on alumina. Rabo et al. (25) observed similar disproportionation of CO on a Ru/SiO_2 system and McCarty and Wise (8) showed in an isotopic exchange study dissociative chemisorption of CO at high

pressure on alumina-supported Ru particles. These results indicate that CO pressure is a decisive factor for the decomposition of CO on Ru although it remains unclear exactly what role it plays.

All particle sizes studied here showed an asymmetric decrease of the CO FTD peak following the various heat treatments, which is due to the loss of higher energy binding sites. The TEM data added clear evidence of faceting during heat treatment which also implies the reduction of lower coordination surface sites. This conclusion is consistent with Wulff's theorem (26) that particles will facet in such a way as to reduce the total surface free energy of the particles as they approach their equilibrium structure. The strong particle size dependence of these changes is probably caused by enhanced particle mobility on the support surface and particle refaceting (surface self diffusion).

The loss of surface oxygen and subsequent revival of the CO desorption peak during annealing of O_2-dosed particles is also noteworthy. We assume that during heat treatment, oxygen (chemisorbed at 50 C) diffuses into the bulk of the Ru, producing clean Ru sites capable of CO adsorption. This type of oxygen diffusion has been observed on single crystal Ru by Lee et al. (27) and Reed et al. (2).

In summary, we have observed no evidence of C decomposition on particulate deposits of Ru on mica at pressures of 10^{-11} to 10^{-6} Torr and temperatures of 300 to 550 K, respectively. However, we have observed significant changes of particle morphology and state of particle dispersion induced by gas and heat treatments which in turn can strongly influence the adsorption and desorption of CO from supported Ru.

ACKNOWLEDGMENTS

We would like to thank Dale Doering and Miguel Avalos-Borja for their assistance in these experiments. Funds for the support of this study have been allocated by NASA-Ames Research Center under Interchanges No. NCA-OR840-002 and NCA-OR840-102.

REFERENCES

1. T. E. Madey and D. Menzel, Jap. J. Appl. Phys. Suppl. 2 (1974), 229.
2. P. D. Reed, C. M. Comrie, and R. M. Lambert, Surf. Sci. 59 (1976), 33.
3. J. C. Fuggle, E. Umbach, P. Feulner, and D. M. Menzel, Surf. Sci. 64 (1977), 64.
4. D. W. Goodman, T. E. Madey, M. Ono, and J. T. Yates, Jr., J. of Catal. 50 (1977), 279.
5. R. Ku and N. A. Gjostein, Surf. Sci. 64 (1977), 465.
6. G. E. Thomas and W. H. Weinberg, J. Chem. Phys. 70 (1979), 1437.
7. G. G. Low and A. T. Bell, J. of Catal. 57 (1979), 397.
8. J. G. McCarty and H. Wise, Chem. Phys. Lett. 61 (1979), 323.
9. D. L. Doering, J. T. Dickinson, and H. Poppa, J. of Catal. 73 (1982), 91.
10. D. L. Doering, H. Poppa, and J. T. Dickinson, J. of Catal. 73 (1982), 104.
11. M. Thomas, J. T.Dickinson, H. Poppa, and G. M. Pound, J. Vac. Sci. Technol. 15 (1978), 568.
12. Yu G. Morozov, A. M. Kostygov, V. I. Petinov, and P. E. Chizhov, Sov. J. Low Temp. Phys. 1 (1975), 674; Phys. Rev. 82 (1951), 87.
13. H. Pfnuer, P. Feulner, H. A. Engelhardt, and D. Menzel, Chem. Phys. Lett. 59 (1978), 481.
14. T. E. Madey, H. A. Engelhardt, and D. Menzel, Surf. Sci. 48 (1975), 304.
15. R. Anton, K. Heinemann, and H. Poppa, Proc. of 8th Int. Vac. Congr. 1 (1980), 121.
16. E. Ruckenstein and Y. F. Chu, J. of Catal. 59 (1979), 109.
17. T. Wang and L. D. Schmidt, submitted to J. of Catal.
18. D. L. Doering, H. Poppa, and J. T. Dickinson, J. Vac. Sci. Technol. 20 (1982), 827.

19. G. Broden, T. N. Rhodin, C. Brucker, R. Benbow, and Z. Hurych, Surf. Sci. 59 (1976), 593.

20. G. Blyholder, J. Phys. Chem. 68 (1964), 2772.

21. G. Doyen and G. Ertl, Surf. Sci. 43 (1974), 197.

22. R. Van Hardeveld and F. Hartog, Surf. Sci. 15 (1969), 189.

23. K. J. Singh and H. E. Grenga, J. Catal. 47 (1977), 328.

24. D. W. Goodman, R. D. Kelley, T. E. Madey, and J. M. White, J. Vac. Sci. Technol. 17 (1980), 143.

26. C. Herring, Phys. Rev. 82 (1951), 87.

27. H. I. Lee, G. Praline, and J. M. White, Surf. Sci. 91 (1980), 581.

FIGURE CAPTIONS

Fig. 1. Transmission electron micrographs of as-deposited particulate Ru films.

a) 30 s — 5 Hz deposit: average particle diameter, $\langle d \rangle$ = 1.2 nm, particle number density, n = $3.7 \times 12^{12}/cm^2$.

b) 150 s — 25 Hz deposit: $\langle d \rangle$ = 2.8 nm, n = $3.4 \times 10^{12}/cm^2$.

c) 300 s — 50 Hz deposit: $\langle d \rangle$ = 6.0 nm, n = $1.3 \times 10^{12}/cm^2$.

d) Transmission Electron Diffraction pattern for deposit b). The sharp reflections are due to diffraction from the mica. The more diffuse and slightly arced spots with sixfold symmetry are from Ru; they are in good registry with the mica pattern, indicating strong epitaxy.

Fig. 2. CO desorption spectra for a series of CO exposures on a 150 s — 50 Hz Ru deposit. The CO adsorption temperature was 320 K.

Fig. 3. Initial CO desorption spectra for different average particle size Ru deposits: (1) 1.2 nm, (2) 2.8 nm, and (3) 6.0 nm. All CO exposures were 6.0 L. Curve 1) has been magnified by a factor of 4 to better show its shape and peak position.

Fig. 4. Three successive CO FTD spectra for a 300 s — 50 Hz Ru deposit of $\langle d \rangle$ = 6.0 nm; CO dose = 6.0 L.

Fig. 5a. Effect of repeated heat treatments (350 C, 35 min.) on the CO desorption spectra for a 30 s — Hz Ru deposit; CO dose = 6.0 L.

Fig. 5b. Heat treatment (350 C, 35 min.) induced decay in CO FTD peak area (in percent FTD peak area loss per flash) vs. particle size.

Fig. 6. Pairs of transmission electron micrographs illustrating the sintering effect of a heat treatment (350 C, 35 min.) on the Ru particles for two deposits: a c (150 s — 25 Hz); b d (300 s — 50 Hz).

Fig. 7. The effect of O_2 preexposure on standard (6L) CO FTD spectra for a 30 s — 5 Hz Ru deposit for: 1) no O_2 (6L), 2) 0.3L of O_2, 3) 3L of O_2, and 4) 6L of O_2. Curve 4) (dashed) peak recovery produced by a heat treatment of 35 min. at 350 C, CO (6L).

Fig. 8. Transmission electron micrographs showing the effect of heat treatment in O_2 (1×10^{-7} Torr for 35 minutes at 350 C) for two Ru deposits: a c (60 s — 10 Hz) and b d (150 s — 25 Hz).

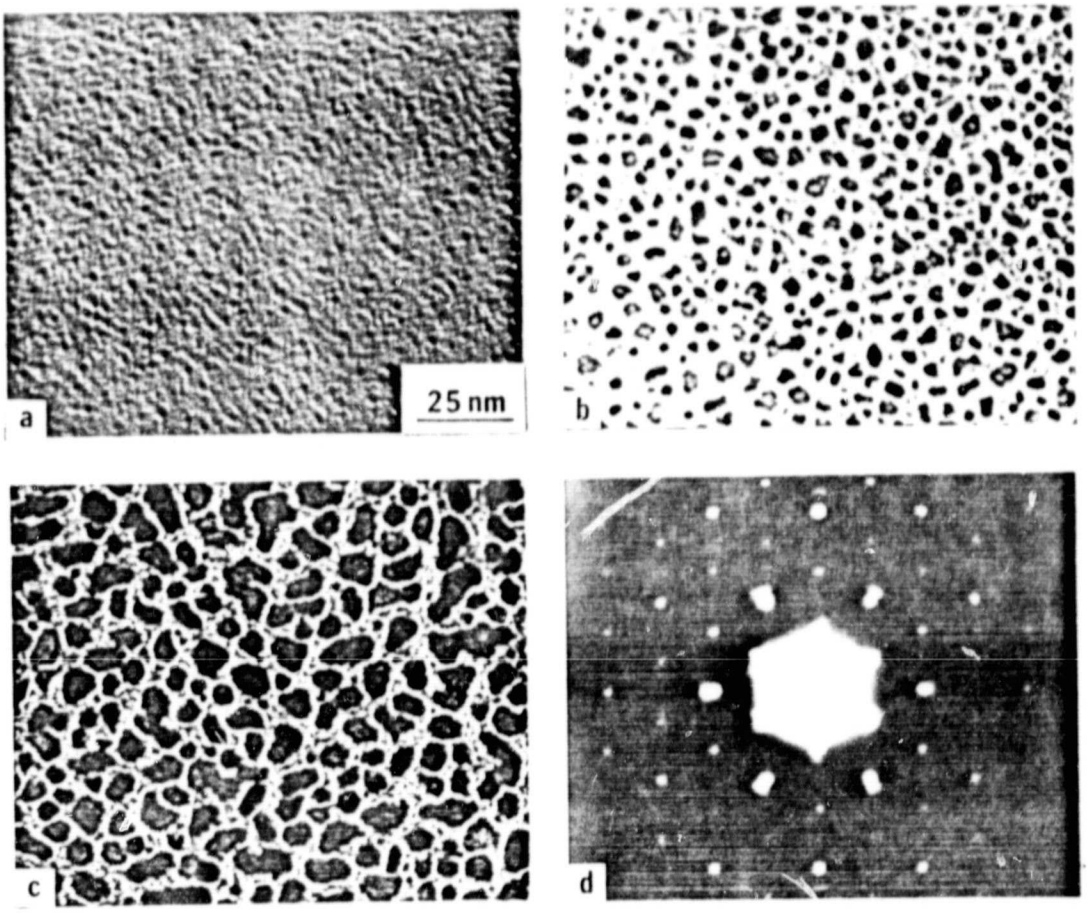

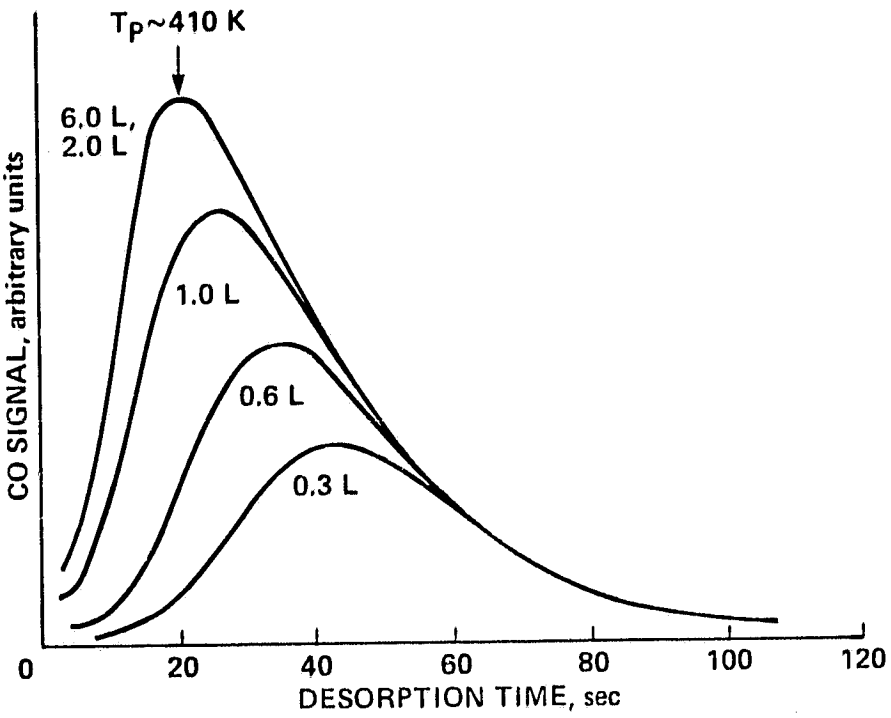
T_P~410 K
6.0 L,
2.0 L
1.0 L
0.6 L
0.3 L
CO SIGNAL, arbitrary units
0
20
40
60
80
100
120
DESORPTION TIME, sec

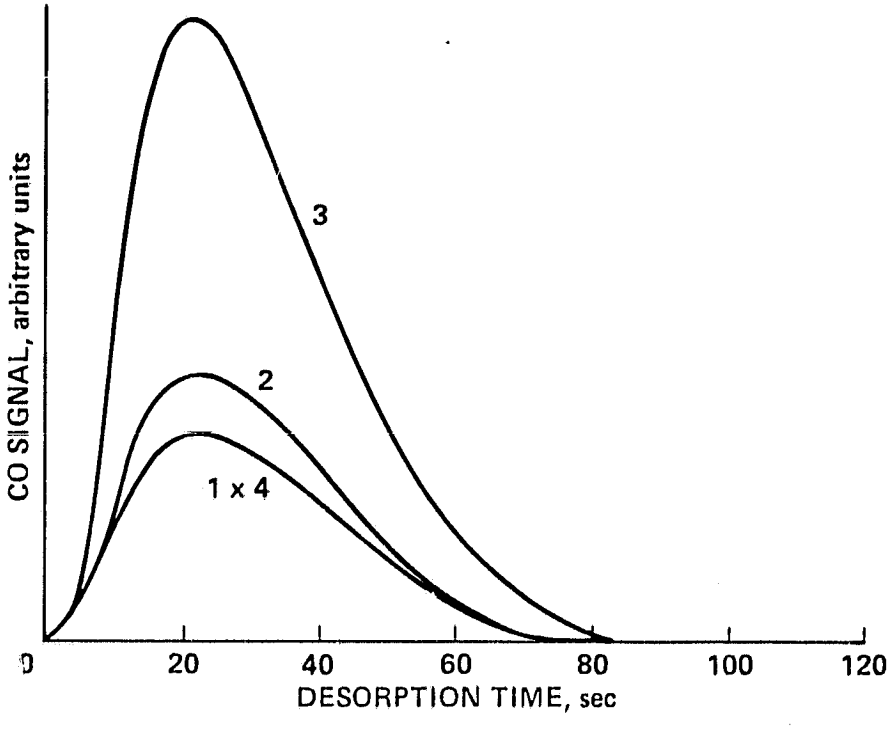
CO SIGNAL, arbitrary units
3
2
1 x 4
0
20
40
60
80
100
120
DESORPTION TIME, sec

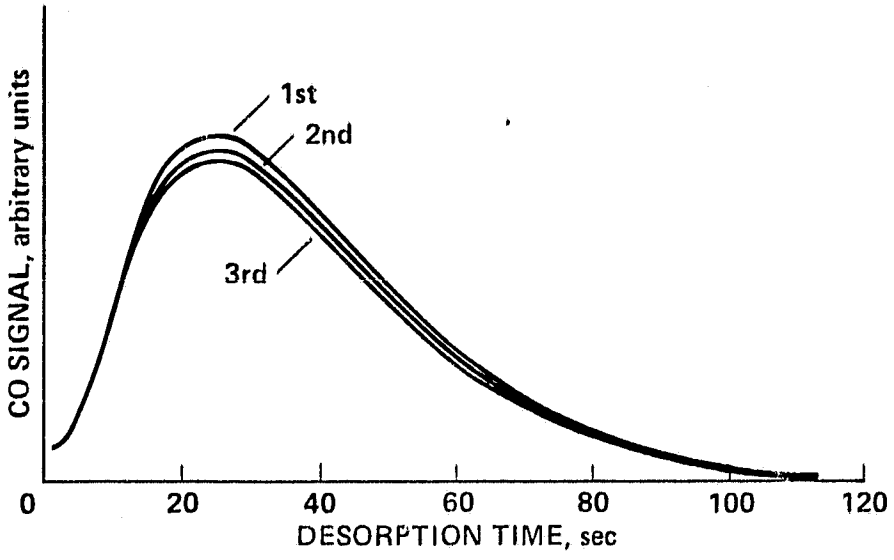
CO SIGNAL, arbitrary units
1st
2nd
3rd
0
20
40
60
80
100
120
DESORPTION TIME, sec

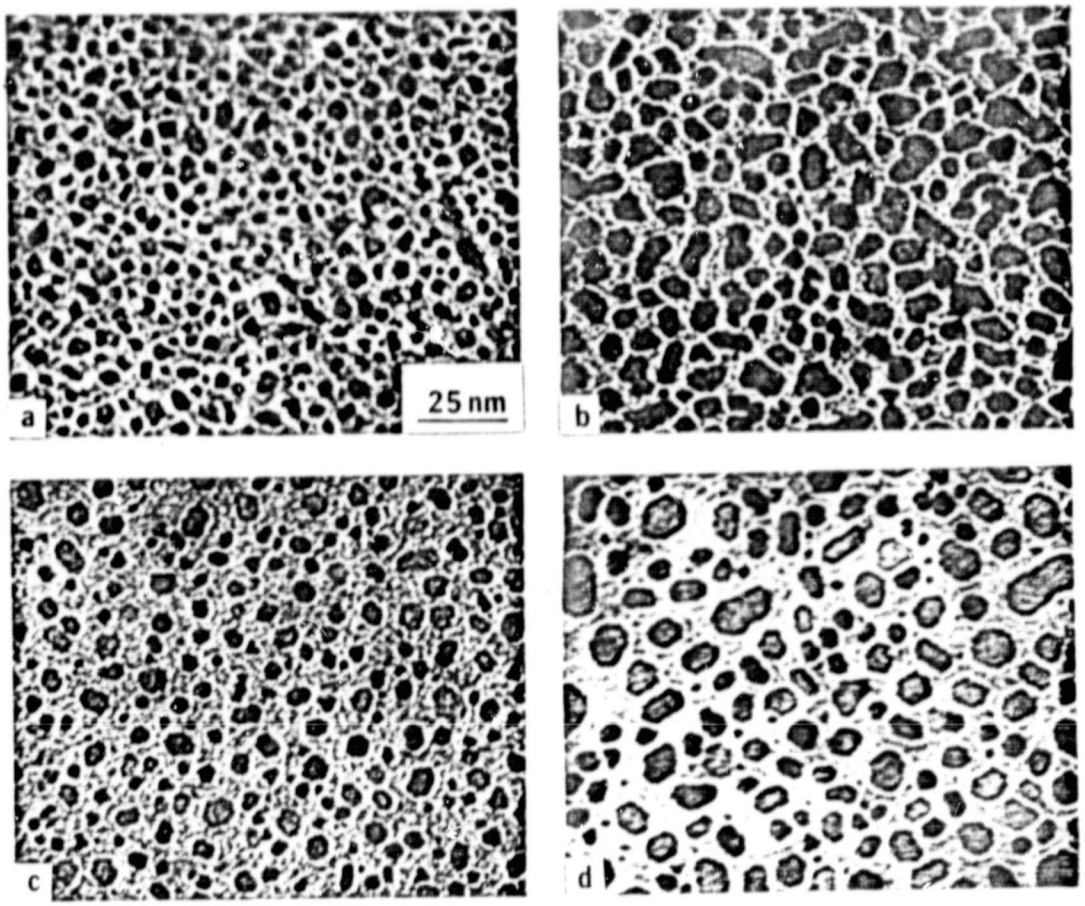

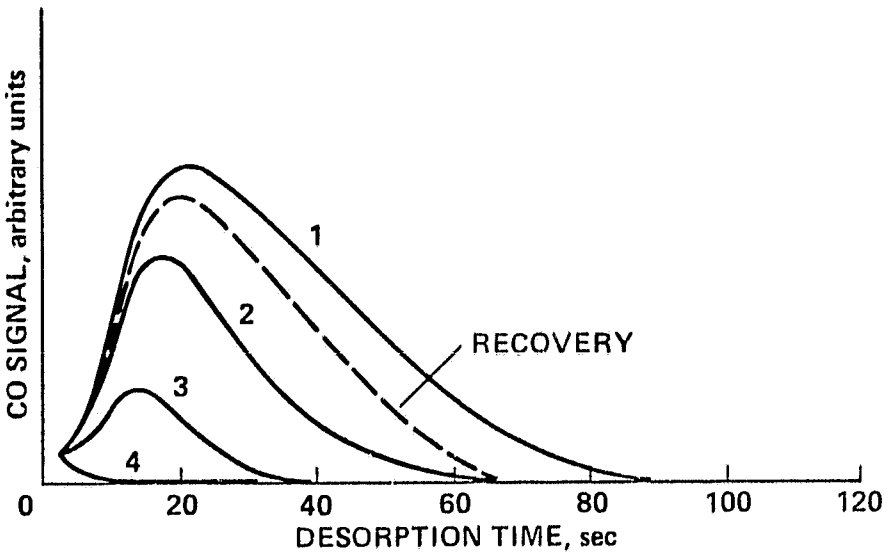
CO SIGNAL, arbitrary units
1
2
3
4
RECOVERY
0
20
40
60
80
100
120
DESORPTION TIME, sec

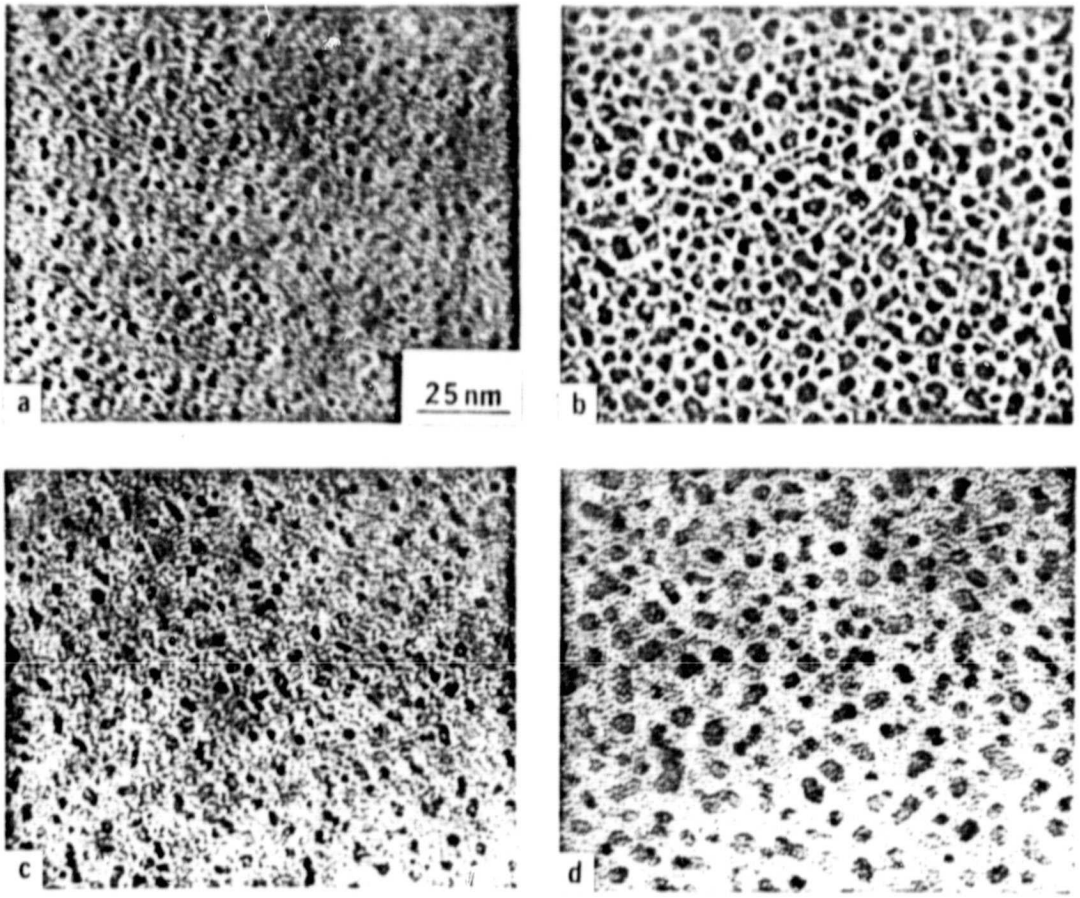

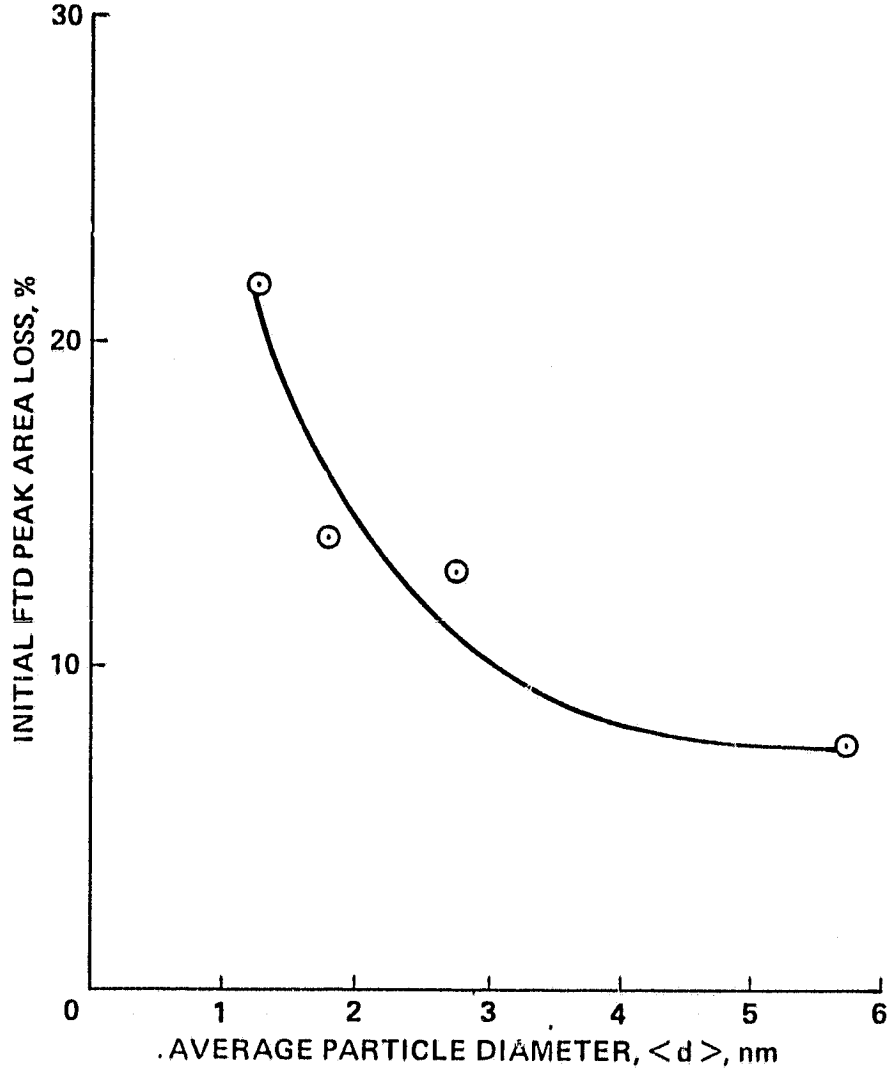
30
20
10
0
1
2
3
4
5
6
INITIAL FTD PEAK AREA LOSS, %
AVERAGE PARTICLE DIAMETER, <d>, nm

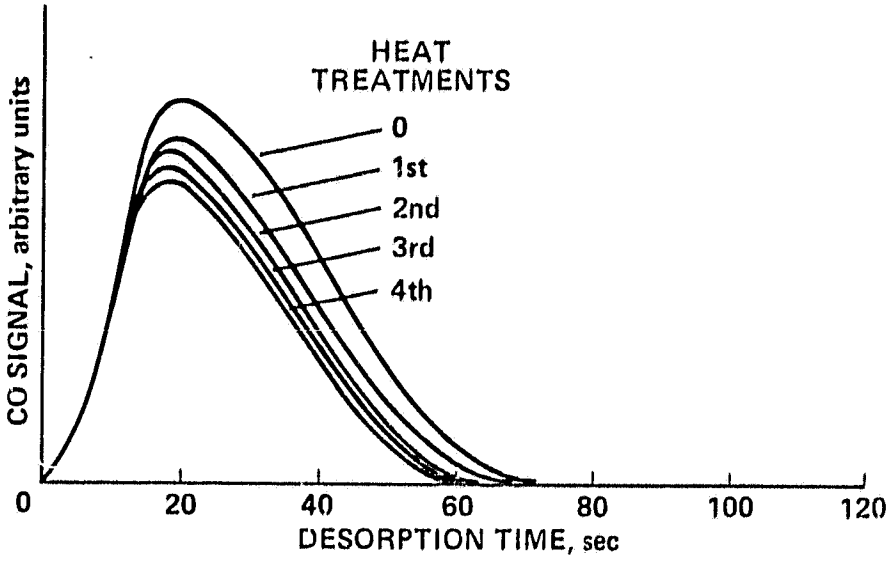
HEAT
TREATMENTS
0
1st
2nd
3rd
4th
CO SIGNAL, arbitrary units
0
20
40
60
80
100
120
DESORPTION TIME, sec